



## Characterization of radio frequency heating of fresh fruits influenced by dielectric properties

S.L. Birla, S. Wang, J. Tang\*, G. Tiwari

Department of Biological Systems Engineering, Washington State University, 213 LJ Smith Hall, P.O. Box 646120, Pullman, WA 99164-6120, USA

### ARTICLE INFO

#### Article history:

Received 29 January 2008

Received in revised form 29 April 2008

Accepted 3 May 2008

Available online 24 May 2008

#### Keywords:

Dielectric properties

Radio frequency

Electromagnetic field

Heating uniformity

Heat treatment

Quarantine

### ABSTRACT

Because of its fast and volumetric nature, radio frequency (RF) heating has been looked upon as a way to overcome the problems associated with conventional heating methods used for disinfestation of fruits. But non-uniform heating within fruits is a major obstacle in adaptation of this technology. In this study, RF heating patterns influenced by dielectric properties (DPs) of fruits were investigated both experimentally and mathematically. A computer simulation model was developed using FEMLAB 3.4, a commercial software for solving Maxwell's electromagnetic and Fourier's heat transfer equations. Orange, apple, grapefruit, peach, and avocado fruits, selected for these studies were subjected to RF heating in a water filled container equipped with a mechanism to keep fruits rotating and moving during RF heating in a 27.12 MHz, 12 kW parallel plate RF unit. DPs of constitutional parts of the selected fruits were measured by open-ended coaxial probe method. The study showed that dissimilarity in peel and pulp DPs greatly influenced the RF heating behavior of the fruits. Core heating was prominent in apple, peeled orange and grapefruit; whereas subsurface/peripheral heating in whole oranges and grapefruit, and avocado. The computer model was an effective tool in characterizing and explaining the heating patterns in the fruits based on DPs. The study helped in better understanding the complex RF heating characteristics of fruits, which may be useful in assessing the design feasibility of product specific RF energy based treatment protocol.

© 2008 Elsevier Ltd. All rights reserved.

### 1. Introduction

Interstate and international trade regulations require postharvest treatments of many fresh fruits to ensure quarantine security from insect pests. Methyl bromide fumigation is the most effective quarantine method for those fruits, but it poses a serious environmental health hazard. Therefore, its use is being phased out under international agreements. Many researchers have explored methods such as thermal treatments by hot water or air, irradiation and cold or controlled atmosphere storage as possible replacement for the chemical decontamination. All these methods have one or other limitations. For example, conventional heating, such as hot water or hot air, is slow as it relies on conduction within fruit. Because of fast and volumetric nature of radio frequency (RF) heating, it has been looked upon as a way to overcome the problems associated with conventional heating methods used for disinfestation of fruits (Hallman and Sharp, 1994; Tang et al., 2000). Nelson (1996) reviewed the research work and concluded that non-uniform heating of fruits was the major stumbling block in the possible use of RF energy for fruit disinfestation. Recently, research has

been conducted to improve the electromagnetic heating uniformity and develop treatment protocols for some commodities, e.g. microwave (MW) energy for cherries (Ikediala et al., 1999) and RF energy for apples (Wang et al., 2006), cherries (Ikediala et al., 2002) and in-shell walnuts (Wang et al., 2001a, 2007). Birla et al. (2004) demonstrated a significant improvement in heating uniformity of fruits when fruits were immersed in water and kept moving and rotating during RF heating. However, they observed differential RF heating rates of water and fruit because of difference in dielectric properties (DPs) of these materials.

DPs referred as permittivity influence reflection of electromagnetic waves at interfaces and the attenuation of the wave energy within materials. The complex relative permittivity  $\epsilon^* = \epsilon' - j\epsilon''$  of a material includes dielectric constant ( $\epsilon'$ ) which represents stored energy when the material is exposed to an electric field, and the dielectric loss factor ( $\epsilon''$ ) which influences energy absorption and attenuation. The RF power absorption in any material is directly proportional to the loss factor, therefore dissimilar materials exposed to similar RF field would heat differently (Ryyänen, 1995). The dielectric loss factor in RF range is dominated by ionic conductance (Guan et al., 2004). Addition of salt in water increases the ionic conductivity and the loss factor (Tang, 2005). The differential heating of fruit and water can be overcome by adding table salt to water (Ikediala et al., 2002). The amount of salt to be added

\* Corresponding author. Tel.: +1 509 335 2140; fax: +1 509 335 2722.  
E-mail address: [jtang@mail.wsu.edu](mailto:jtang@mail.wsu.edu) (J. Tang).

**Nomenclature**

$C_p$	specific heat ( $\text{J kg}^{-1} \text{K}^{-1}$ )	$t$	time (s)
$d$	thickness, (m)	$V$	electric potential (V)
$E$	electric field strength ( $\text{V m}^{-1}$ )	<b>Greek symbols</b>	
$f$	frequency (Hz)	$\rho$	density ( $\text{kg m}^{-3}$ )
$h$	heat transfer coefficient ( $\text{W m}^{-2} \text{K}^{-1}$ )	$E'$	dielectric constant
$j$	complex number operator	$E''$	dielectric loss factor
$k$	thermal conductivity ( $\text{W m}^{-1} \text{K}^{-1}$ )	$\epsilon_0$	permittivity of free space ( $\text{F m}^{-1}$ )
$Q$	power density ( $\text{W m}^{-3}$ )	$\nabla$	delta operator
$T$	temperature (K)		

depends upon the DPs of the fruit. Therefore information of DPs of fruits is essential for proper design of RF heating processes.

Information on DP data for many fruits has been published over the last decade (Foster and Schwan, 1989; Nelson, 1996; Ryyänen, 1995; Venkatesh and Raghavan, 2004; Wang et al., 2005). Nelson (2003) reported temperature and frequency dependent DPs of several fresh fruits and vegetables in 0.01–1.8 GHz frequency range. Sipaghioglu and Barringer (2003) expressed DPs of fruits and vegetables as a function of temperature, ash, and moisture content. Seaman and Seals (1991) measured the DPs (0.15–6.4 GHz) of peel and pulp of apples and oranges at room temperature and they reported a large difference in DPs between pulp and peel. However, no data have been reported for fruit peel at 27.12 MHz frequency. It is crucial to measure DPs of each fruit constituent part such as peel and pulp for understanding how the DPs influence the RF heating patterns.

RF heating characteristics of fruits are not just influenced by DPs but also by fruit shape and size, the surrounding medium and relative distance between fruit and the two electrodes (Birla et al., 2008). Moreover temperature dependant DPs make it impossible to obtain analytical solutions for the coupled Maxwell and Fourier equations, which govern the electric field distribution and heat diffusion inside the material, respectively. A computer program is highly advantageous to solve coupled non-linear equations. Such computer model was developed in earlier our work (Birla et al., 2008) for studying the RF heating characteristic of homogenous model fruit immersed in water. The model can be modified to simulate heating patterns in real fruits which are not homogenous but consist of stratified layers of peel, pulp and stone.

The objectives of this study were to: (1) measure DPs of peel and pulp of selected fruits, (2) modify and validate the computer model for characterization of RF heating of stratified model fruit, (3) apply the computer model to provide insight into how the DPs of fresh fruits influence heating pattern. The characterization of fruit heating patterns based on DPs would help in understanding the complex nature of RF heating, which is necessary for assessing the potential problems and suggesting ways and means to develop effective RF treatment protocols for fresh fruits.

## 2. Materials and methods

Systematic characterization of RF heating of fruits requires appropriate information of dielectric and thermal properties of fruits peel and pulp in the computer model. Following sections describe the DPs measurement and computer modeling procedures.

### 2.1. DPs measurement

'Red delicious' and 'golden delicious' apples (*Malus sylvestris*), 'navel' and 'valencia' oranges (*Citrus sinensis* L. Osbeck), 'marsh' grapefruit (*Citrus perdesi* Macfad.), 'gwen' avocado (*Persea ameri-*

*cana*), and 'elegant lady' peach (*Prunus persica*) were purchased from local grocery store for measuring DPs of pulp and peel of these fruits, and for studying the RF heating pattern. These fruits were selected to cover the wide varieties of spherical fruits, which could be easily moved and rotated in the fruit mover designed in our earlier study (Birla et al., 2004) for improving RF heating uniformity.

DPs of the selected fruits were measured between 1 MHz and 1800 MHz. This frequency range covers three US Federal Communications Commission (FCC) allocated RF frequencies (13, 27, and 40 MHz) and one microwave frequency (915 MHz) for industrial heating applications. The upper frequency (1800 MHz) is close to another FCC allocated frequency 2450 MHz, mainly used in domestic microwave ovens. The measurement system consisted of an open ended dielectric probe connected with an impedance analyzer (Model 4291B, Agilent Technologies, Santa Clara, CA, USA) which is interfaced with a personal computer (Fig. 1). Prior to the measurement, the system was calibrated following prescribed standard procedure (Wang et al., 2003a,b). Reliability of the measurement system was assessed by measuring DPs of butyl alcohol at 20 °C and compared with literature values. Typical measurement error of the system was about 5%. Each measurement was repeated three times and results were reported as mean values.

As DPs of biological materials are, in general, temperature dependent, it is highly desirable to measure the DPs of the material at different temperatures which cover the range of intended applications of dielectric heating. Wang et al. (2003b) used a custom designed sample holder to measure the DPs of fruit pulps of apple, orange, grapefruit, and avocado at varying temperatures. In the designed sample holder, fruit pulp tissue need to be shredded/grated or pureed to maintain proper contact with the probe. Birla (2006) used the sample holder to measure orange peel properties at different temperatures. Preliminary observations showed that minced peel sample was more compact than the intact tissue because of air exclusion during mincing. For fruit peel such as orange rind which is porous and filled with small pockets of air, this sample preparation method might damage the tissue structure

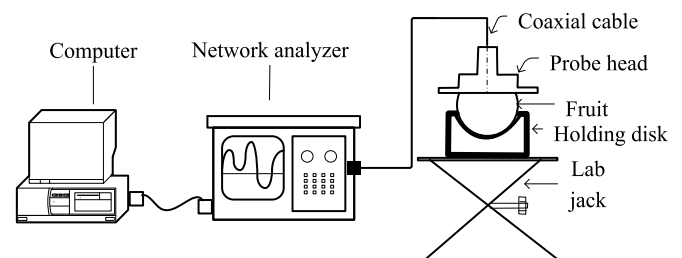


Fig. 1. Experimental setup for dielectric properties measurement (Not to scale).

and possibly alter the DPs of the specimen. Moreover in case of apple and peach, the thin peel of fruit made it very difficult to prepare sample. Preliminary measurement using such prepared fruit samples suggested a significant change in DP's of peel tissues; hence measurements were made on intact peel and pulp tissues at room temperature.

The fruit sample was secured on a laboratory mini-support jack to ensure that flat and smooth surface of the sample was in close contact with the probe (Fig. 1). For avocado, outer rough peel surface was smoothened by scrapping off a thin layer to have intimate contact of probe face and peel surface. In case of pulp tissue property measurement, fruits were halved equatorially and cut surfaces brought in close contact with the probe. Care was taken to avoid undue pressure on the tissue which could lead to deformation of the tissues and juice oozing. DPs of orange and grapefruit peel were measured for both flavedo and albedo layers of peel. The outer flavedo layer contains volatile compounds whereas inner layer albedo is a spongy white fibrous material.

## 2.2. Model fruit preparation

Difficulty in measuring temperature dependent DPs of fresh fruit peels necessitated the need to develop a stratified model fruit from the materials whose temperature dependent DPs are well known or can be determined easily. The model fruit can be used for validation of computer model that would be used for developing better understanding of internal heating pattern in the fruit as influenced by the DPs of fruit constituent's parts.

In our previous study (Birla et al., 2008), a model fruit made from 1% gellan gel (GG) was used for validating a computer simulation model for homogenous subject. In reality, fruit is composed of two dissimilar layers. Hence, to make a stratified model fruit, there was a need to choose a material whose dielectric constant is vastly different from that of gellan gel ( $\epsilon' = 84$  at 27.12 MHz) and also can form stable and firm structure. Whey protein gel (WPG) ( $\epsilon' \sim 100$  and  $\epsilon'' \sim 800$  at 27.12 MHz and 20 °C) has been used as a model food system for validation of microwave sterilization process of fish fillets (Chen et al., 2007). The dielectric loss factor of WPG can be increased by addition of table salt without much affecting the dielectric constant (Wang et al., 2003c). A stratified model fruit can be produced using WPG for the inner core formation and GG as the outer peel. Contrast in DP's of these two materials should provide clear understanding of the effect of peels. Both homogenous and stratified model fruits made from WPG and GG were used for validating and studying the effect of peel and pulp DPs on RF heating patterns.

The model fruits were formed using two polypropylene moulds of 70 and 80 mm internal diameters consisted of two hemispherical halves. The whey protein mixture (Alacen 882 containing 80% whey protein concentrate, New Zealand Milk Products, Santa Rosa, CA), 2% glucose (Fisher Scientific, Fair Lawn, NJ), 0.59% sodium chloride were dissolved in distilled water. The mixture was stirred

for 1.5–2 h at room temperature on a magnetic stirring device for complete dispersion of whey protein powder. To make homogenous model fruit, whey protein solution was poured in 70 and 80 mm dia moulds and sealed using cello-tape. Moulds were put in the 90 °C water bath for 2 h to set the gel. One percent gellan gum (Kelcogel, Kelco Division of Merck and Co., San Diego, CA) was dissolved in deionized water and the solution was heated to 90 °C in 15 min (Tang et al., 1995). At 20 °C,  $\epsilon'$  of fresh fruits pulp varies from 70 to 90 and  $\epsilon''$  varies from 120 to 220 (Wang et al., 2003b), hence 0.17%  $\text{CaCl}_2$  salt was added into the hot gellan gum solution to bring the loss factor to this range. Hot gel solution was poured into the 80 mm mould through a hole in one half and allowed to cool at room temperature for 30 min to ensure gel setting and easy removal of the ball (Tang et al., 1997). To make the stratified fruit, the formed 70 mm dia whey gel ball was secured in-place at the geometric centre of the 80 mm mould using a steel rod (5 mm dia 90 mm long). The rod passed through the center of the gel ball, with both ends resting on the 80 mm mould edge. The DPs of 1% gellan gel reported by Wang et al. (2003a) and WPG properties reported by Wang et al. (2003b) were used in the computer simulation (Table 1).

## 2.3. Procedure for RF heating pattern determination

The homogenous and stratified model fruits made from GG and WPG were subjected to RF heating in a fruit mover for validation of computer simulation results. The selected fruits (apple, orange, grapefruit, avocado, and peach) were stored at room temperature in sealed bags for 12 h to attain equilibrium room temperature ( $\sim 20$  °C). One fruit from each cultivar/class was randomly picked and eight assorted fruits were grouped. Another similar group of eight assorted fruits were peeled off to study the effect of peel on RF heating pattern. The RF heating of the selected fruits batches and the model fruits was conducted in a 12 kW, 27.12 MHz batch type RF heating system (Strayfield Fastran with E-200, Strayfield International Limited, Wokingham, UK). The batch of the fruits was placed in a tap water filled fruit mover developed in the previous study (Birla et al., 2004). Fig. 2 shows the schematic diagram of the fruit mover system placed in 200 mm RF electrodes gap. The assorted fruits were kept in motion by means of water jet nozzles mounted on the periphery of the fruit mover. A thermocouple thermometer installed in a water circulation pipe monitored the water temperature during RF heating (Fig. 2). The RF input power was switched off when the water temperature reached 50 °C. Details of the fruit mover and operating procedure have been explained elsewhere (Birla et al., 2004). Immediately after RF heating, the fruits were halved equatorially and thermal images of one-half cut section of the fruits were recorded using an infrared imaging camera (ThermaCAM<sup>TM</sup> Researcher 2001, accuracy  $\pm 2$  °C, five picture recordings per second, FLIR Systems, Portland, OR).

**Table 1**  
Electrical and physical properties of the materials used in simulation

Material	Thermal conductivity $k$ , $\text{W m}^{-1} \text{K}^{-1}$	Density $\rho$ , $\text{kg m}^{-3}$	Specific heat $C_p$ , $\text{J kg}^{-1} \text{K}^{-1}$	Dielectric constant ( $\epsilon'$ ) <sup>a</sup>	Loss factor ( $\epsilon''$ ) <sup>a</sup>
Gellan gel	0.53	1010	4160	$-0.21T + 86.76$	$4.36T + 129.4$
Whey protein gel <sup>b</sup>	0.55	1050	3850	$0.28T + 93.56$	$17.51T + 468.23$
Tap water	0.56	1000	4180	$-0.48T + 84.74$	$0.33T + 11.1$
Orange (pulp)	0.58	1030	3661	$-0.22T + 88.6$	$4.9T + 122.6$
Orange (peel)	0.40	800	3300	$-0.16T + 82.53^c$	$3.94T + 58.2^c$
GD apple (pulp)	0.51	845	3800	$-0.14T + 74.9$	$2.87T + 59.2$
Grapefruit (pulp)	0.54	950	3703	$0.17T + 85$	$5.01T + 95.21$
Avocado (pulp)	0.42	1060	3380	$0.63T + 104.36$	$14.47T + 393.94$

Source: <sup>a</sup>DP: (Wang et al., 2003a,b,c), <sup>b</sup>(Chen et al., 2007)  $T$  – Temperature, °C, physical properties from (Rehman, 1995), <sup>c</sup>orange peel DP from (Birla, 2006).

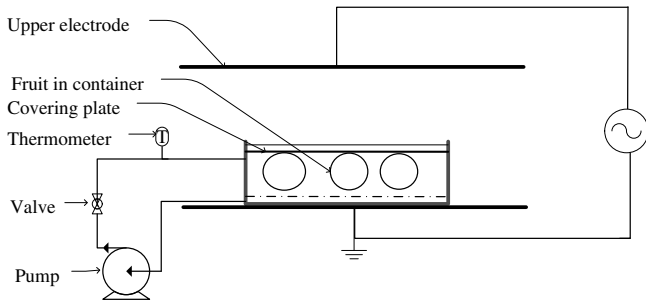


Fig. 2. Schematic diagram of the RF heating system equipped with a fruit mover.

#### 2.4. Characterization of RF heating of fruit

A computer model developed in our previous study (Birla et al., 2008) was modified as explained below for simulation of RF heating of the model fruits and characterization of fresh fruit heating pattern.

##### 2.4.1. Governing equations

In our previous simulation model, Navier–Stoke's equations were solved to take into account the influence of convective heat transfer in the fluid domain. Solving coupled electromagnetic (EM) field and Navier–Stoke's equations requires a large computer memory and, sometimes, convergence is an issue. In this study, we were interested in studying the effect of DPs of fruit on heating patterns, hence solution of coupled Fourier heat transfer and quasi-static EM field equations should be sufficient to characterize heating pattern of the fruit.

$$\frac{\partial T}{\partial t} = \frac{k}{\rho C_p} \nabla^2 T + \frac{Q}{\rho C_p} \quad (1)$$

where  $C_p$  is the specific heat ( $\text{J kg}^{-1} \text{K}^{-1}$ ),  $k$  is the thermal conductivity ( $\text{W m}^{-1} \text{K}^{-1}$ ),  $t$  is the heating time (s),  $T$  is the temperature (K), and  $\rho$  is the density ( $\text{kg m}^{-3}$ ).

The absorbed RF power per unit volume ( $Q$ ,  $\text{W m}^{-3}$ ), referred as power density, is governed by electric field strength ( $E$ ,  $\text{V m}^{-1}$ ), dielectric loss factor ( $\epsilon''$ ) and the frequency ( $f$ , Hz) (Choi and Konrad, 1991) as below:

$$Q = 2\pi f \epsilon_0 \epsilon'' E_{\text{rms}}^2 = \pi f \epsilon_0 \epsilon'' |\mathbf{E}|^2 \quad (2)$$

where  $\epsilon_0$  is the permittivity in free space ( $8.85 \times 10^{-12} \text{ F m}^{-1}$ ), and  $E_{\text{rms}}$  is the root mean square value of the electric field which is equal to  $1/\sqrt{2}$  times of the  $E$ -field amplitude. The scalar voltage potential ( $V$ , V) is related to the electric field as  $E = -\nabla V$ . The voltage potential at any point inside the electrodes is governed by Eq. (3) which was derived from a quasi-static approximation of Maxwell's equations (Choi and Konrad, 1991):

$$-\nabla \cdot ((2\pi f \epsilon_0 (\epsilon'' + j\epsilon')) \nabla V) = 0 \quad (3)$$

##### 2.4.2. Geometric model and assumptions

The fruit mover container ( $425 \text{ mm} \times 425 \text{ mm} \times 127 \text{ mm}$  made of 6 mm thick HDPE sheet) was placed in a 200 mm gap between two parallel plate electrodes in the RF heating system. Eight spherical fruits (80 mm dia) floated in equal distant along the periphery of the container, 25 mm above the bottom of the container. One fourth of the RF system and fruit mover container was modeled to take advantage of the system symmetry (Fig. 3). Since fruits were continuously moved and rotated during RF heating, simulation of these fruits was very difficult because of the associated moving boundary conditions. For simplification, stratified spherical fruits were assumed to be rotating on their own axes and RF en-

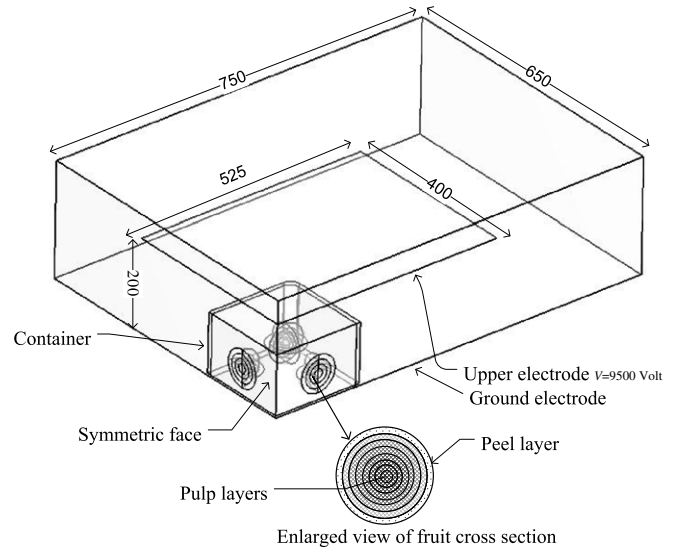


Fig. 3. Geometrical model of one quadrant of RF heating system and 8 fruit immersed in water filled container sandwiched between 200 mm apart electrodes (dimensions are in mm).

ergy absorbed on each layer was uniform. The assumption was based on the occurrence of concentric temperature contours over the cross section of gellan gel model fruit subjected to RF heating in the fruit mover (Birla et al., 2008). Time average power density in each layer was estimated by integrating power density over the individual layer and dividing it by the volume of the layer in each time step. Theoretically the number of layers should be infinite but increase in the number of layers greatly increased the computer memory requirement for integration at each time step. Simulation with eight stratified layers of 5 mm thickness was found to be converging and results were reasonably accurate.

##### 2.4.3. Initial and boundary conditions

Source electric potential 9500 V, as estimated in our previous study (Birla et al., 2008), was applied to the top electrode and symmetric surfaces were assigned thermal and electrical insulating boundary conditions as shown in Fig. 3. The convective heat transfer coefficient was assumed to be  $20 \text{ W m}^{-2} \text{K}^{-1}$  for water–air and container–air interfaces (Wang et al., 2001b). Table 1 summarizes the properties of the model fruit and water used in the simulation. All computer simulations were performed on a Dell 670 work station with two each Dual-Core, 2.80 GHz XEON processors and 12 GB RAM running a Windows XP 64-bit operating system.

##### 2.4.4. Characterization of RF heating of fresh fruits

For validation of the modified model, RF heating patterns of homogenous and stratified model fruits were simulated. RF heating profiles of fresh peeled fruits were also simulated using temperature dependent DP's of fruits pulp reported by Wang et al. (2003b). Table 1 summarizes the material properties used in the simulation. Unavailability of reliable temperature dependent DPs of fruits peel hindered our effort to simulate heating profiles of whole fresh fruits. Temperature dependent DPs of orange peel sample documented by Birla (2006) were used to understand the effect of peel properties. However, to gain insight into the influence of peel properties on heating pattern for other fruits, power density profiles inside the fruits were simulated for varying DPs of the peel with respect to the pulp properties. A graph showing relationship between power density ratio and DPs ratio of fruit peel and pulp was prepared. Values of dielectric constant and loss factor of fresh fruits, obtained in this study were superimposed on the graph to



explain the observed RF heating patterns of the selected fresh fruits.

### 3. Results and discussions

#### 3.1. Dielectric properties

DPs of the fruits at 27.12 MHz frequency were summarized in Table 2 together with DPs at 915 and 1800 MHz, which might be useful for microwave based process design by other researchers. Measured dielectric data for navel orange shown in Fig. 4 confirmed that disruption of biological tissues alters the DPs. The dielectric constant and the loss factor measured at ~20 °C and 27.12 MHz were different for 'navel' orange pulp and intact pulp tissue, minced peel and peel tissue, and juice. The loss factor of the pulp slurry was almost twice that of the peel, but was slightly smaller than that of the juice and the intact pulp tissue. The lower value of the pulp slurry loss factor might be attributed to entrapped air, which was whipped in during pulp slurry sample preparation. The loss factor of the peel tissue was less than that of minced peel, which might be due to expulsion of air from the minced peel while preparing samples. It was corroborated by the observation that the minced peel sample was more compact than the intact tissue. Hence it can be inferred that the spongy peel tissue structure breakdown significantly altered the DPs. As the influence of sample preparation technique on DPs of pulp was less significant, pulp properties measured by Wang et al. (2003b) for orange, apple, and grapefruit pulp samples at temperatures between 20 and 60 °C can be used for simulation.

DPs of intact peel and pulp tissues of the selected fruits measured at 27.12 MHz are shown in Fig. 5. There were differences in DPs among the selected fruits and also between different cultivars. The values of DPs for 'valencia' orange were greater than those of 'navel' orange, which might be caused by the difference in physio-chemical properties such as acidity, total solid contents, juice yield etc. between cultivars. In orange and grapefruit, the outer peel layer, referred as flavedo, contained volatile compounds and coated with natural wax. DP measurement performed on the outer peel surface at 27 MHz revealed that the value of dielectric constant was higher than that of orange pulp (Table 2). The inner most orange peel layer, referred as albedo, had significantly lower values of dielectric constant and loss factor compared with the val-

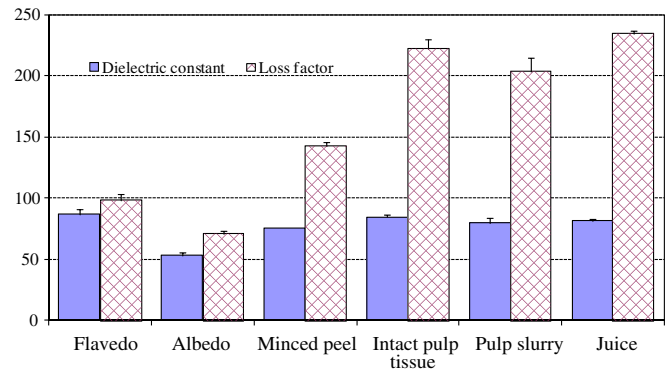


Fig. 4. Dielectric properties of navel orange pulp, minced peel, peel tissue, pulp tissue and juice at 20 °C and 27.12 MHz.

ues for the flavedo layer. This influence of DPs variation in peel and pulp tissues on the heating pattern of fruits will be discussed in Section 3.3.

The dielectric constant and loss factor values of apple peel tissue were very small in comparison with those of pulp tissues. This is in agreement with results reported by Seaman and Seals (1991) in which a large difference was observed between the DPs of pulp and skin of GD apples measured from 150 to 6400 MHz. Similarly in peach, a large difference was observed in DPs between peel and pulp (Fig. 5). Values of both dielectric constant and loss factor of avocado pulp were very high in comparison with other selected fruits. Nelson (2003) and Wang et al. (2005) also reported similar results and attributed this to high oil and salt content in fruit pulp. Low values of avocado peel DPs were attributed to dry skin.

In the open co-axial probe measurement setup, the minimum sample thickness (in mm) requirement to ensure accurate DP measurement is governed by the dielectric constant ( $\epsilon'$ ) of the test sample (Hewlett and Packard, 1996):

$$\text{Thickness (in mm)} = \frac{20}{\sqrt{\epsilon'}} \quad (4)$$

For example, a sample with  $\epsilon'$  value of 81 requires minimum thickness of 2.22 mm to have no effect of the adjacent layer on the DPs measurement accuracy. In case of apple and peach, which

Table 2  
Dielectric properties (mean  $\pm$  STD) of constituent parts of the selected fruits at 27.12, 915 and 1800 MHz frequencies at ~20 °C

Fruit Dia (peel thickness, mm)	Tissue/part	27 MHz		915 MHz		1800 MHz	
		$\epsilon'$	$\epsilon''$	$\epsilon'$	$\epsilon''$	$\epsilon'$	$\epsilon''$
N. orange 79(6)	Pulp	84.57 $\pm$ 4.51	222.48 $\pm$ 11.57	72.16 $\pm$ 3.95	11.61 $\pm$ 0.56	70.56 $\pm$ 4.25	12.21 $\pm$ 0.74
	Flavedo	86.55 $\pm$ 4.56	98.27 $\pm$ 5.21	44.28 $\pm$ 4.43	11.23 $\pm$ 1.14	43.8 $\pm$ 4.12	10.73 $\pm$ 1.47
	Albedo	52.84 $\pm$ 3.04	70.65 $\pm$ 2.87	40.72 $\pm$ 1.95	8.4 $\pm$ 1.05	38.63 $\pm$ 2.25	9.7 $\pm$ 1.52
V. orange 68(4)	Pulp	85.29 $\pm$ 5.52	240.09 $\pm$ 13.88	74.23 $\pm$ 3.12	15.03 $\pm$ 2.31	70.62 $\pm$ 34.03	15.99 $\pm$ 1.92
	Flavedo	95.52 $\pm$ 9.44	99.41 $\pm$ 16.7	43.02 $\pm$ 3.95	10.73 $\pm$ 1.23	40.43 $\pm$ 3.61	10.24 $\pm$ 1.22
	Albedo	48.49 $\pm$ 2.64	68.92 $\pm$ 3.04	38.16 $\pm$ 2.83	7.76 $\pm$ 1.71	35.82 $\pm$ 2.97	8.78 $\pm$ 2.02
Grapefruit 84(8)	Pulp	99.42 $\pm$ 2.77	245.7 $\pm$ 12.81	69.44 $\pm$ 3.79	14.53 $\pm$ 0.47	66.93 $\pm$ 3.82	14.22 $\pm$ 0.08
	Flavedo	65.77 $\pm$ 5.40	161.67 $\pm$ 44.16	51.09 $\pm$ 5.06	12.93 $\pm$ 2.87	48.6 $\pm$ 9.21	11.89 $\pm$ 2.30
	Albedo	44.69 $\pm$ 3.48	83.98 $\pm$ 4.98	27.94 $\pm$ 2.98	7.54 $\pm$ 1.08	25.89 $\pm$ 3.06	7.52 $\pm$ 1.92
GD apple 75(1)	Sub-surface	63.58 $\pm$ 4.79	67.88 $\pm$ 7.63	55.08 $\pm$ 4.20	7.47 $\pm$ 0.72	53.89 $\pm$ 3.46	9.27 $\pm$ 0.69
	Core	84.86 $\pm$ 7.18	132.73 $\pm$ 2.51	65.02 $\pm$ 1.92	12.25 $\pm$ 0.64	62.67 $\pm$ 1.54	12.98 $\pm$ 0.67
	Peel	40.2 $\pm$ 1.30	22.39 $\pm$ 2.94	26.94 $\pm$ 3.51	3.38 $\pm$ 0.59	26.34 $\pm$ 3.32	3.53 $\pm$ 0.78
RD apple 76(1.5)	Sub-surface	62.38 $\pm$ 5.38	67.37 $\pm$ 16.70	55.68 $\pm$ 3.33	7.06 $\pm$ 1.04	54.35 $\pm$ 3.30	8.93 $\pm$ 0.90
	Core	72.31 $\pm$ 2.60	115.44 $\pm$ 5.14	62.14 $\pm$ 0.81	9.28 $\pm$ 0.59	60.64 $\pm$ 0.78	10.38 $\pm$ 0.37
	Peel	38.77 $\pm$ 6.66	23.15 $\pm$ 2.88	28.61 $\pm$ 5.02	3.18 $\pm$ 0.73	28.03 $\pm$ 4.81	3.87 $\pm$ .64
Avocado 58(6)	Pulp	146.73 $\pm$ 16.67	574.71 $\pm$ 75.66	53.1 $\pm$ 3.59	24.09 $\pm$ 2.06	50.95 $\pm$ 3.44	17.08 $\pm$ 1.27
	Stone	4.81 $\pm$ 0.57	0.15 $\pm$ 0.01	4.52 $\pm$ 0.58	0.28 $\pm$ 0.05	4.57 $\pm$ 0.53	0.23 $\pm$ 0.07
	Peel	8.31 $\pm$ 0.37	0.32 $\pm$ 0.09	7.59 $\pm$ 0.08	0.21 $\pm$ 0.06	5.94 $\pm$ 0.04	0.19 $\pm$ 0.03
Peach 65(0.7)	Pulp	90.09 $\pm$ 7.87	269.5 $\pm$ 45.96	76.32 $\pm$ 5.64	16.12 $\pm$ 2.12	72.14 $\pm$ 3.87	16.4 $\pm$ 3.18
	Peel	85.06 $\pm$ 3.03	213 $\pm$ 5.66	74.34 $\pm$ 3.83	12.5 $\pm$ 2.31	68.12 $\pm$ 2.87	13.1 $\pm$ 2.92

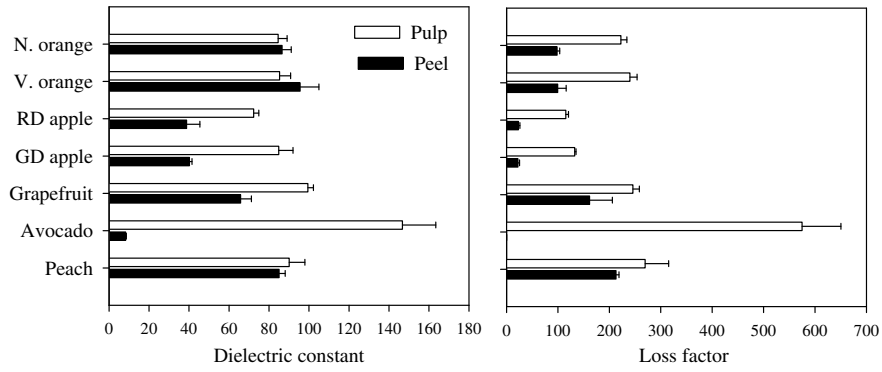


Fig. 5. Dielectric properties of peel (Flavedo) and pulp tissues of the selected fruits measured at 27.12 MHz and 20 °C.

have very thin peel, Eq. (4) may not be satisfied. Hence, the measured values were used only for comparative purposes.

3.2. Characterization of RF heating patterns in model fruits

First, RF heating of homogenous model fruits made of GG and WPG was conducted in the fruit mover (which was placed in

200 mm electrodes gap) to validate the computer simulation model developed for providing insight into heating pattern as influenced by DPs.

Fig. 6 shows both, the simulated and the experimental temperature profiles, at a cross section that cut through the core of the fruit. Temperature rise from initial temperature of 20 °C in 6 min was higher in GG model fruit (60 °C) than WPG model fruit

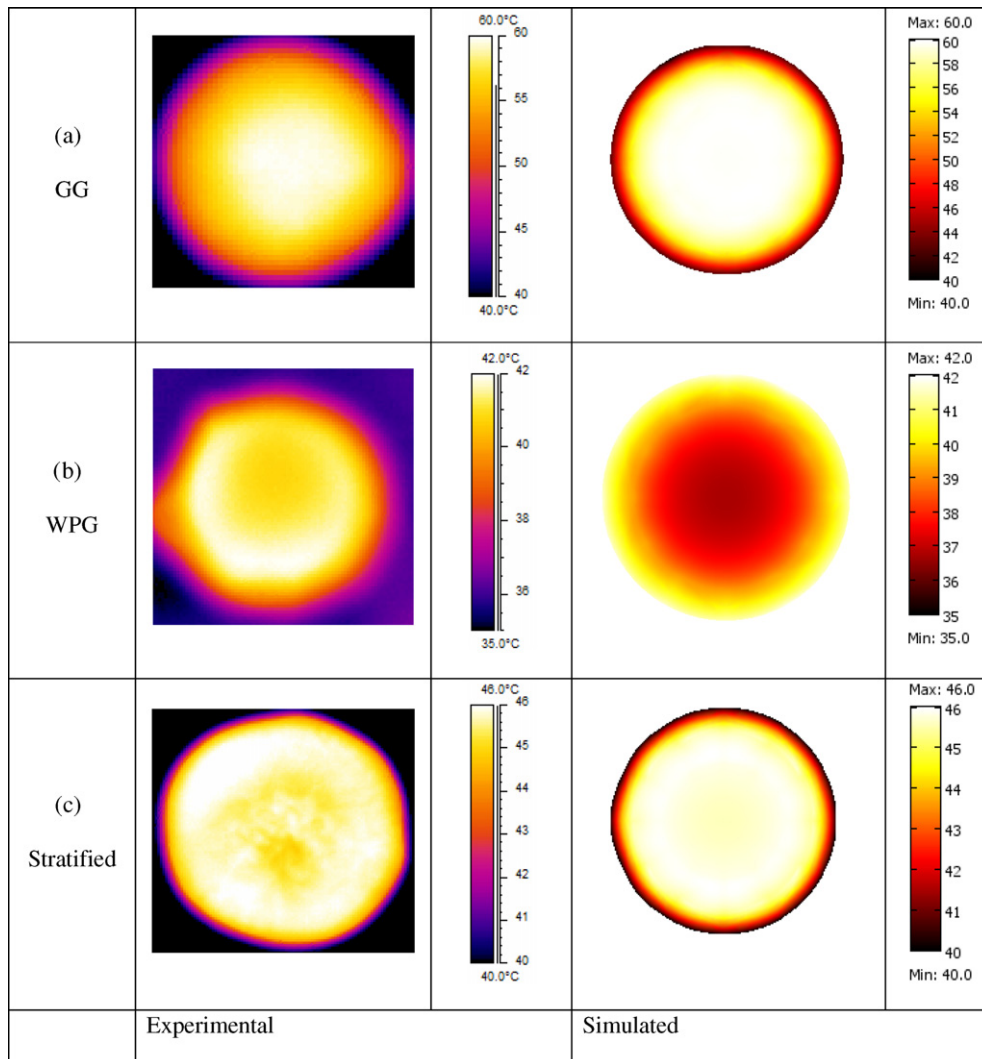


Fig. 6. Simulated and experimental heating patterns in homogenous and stratified spherical model fruit (80 mm dia) made from gellan gel (GG) and whey protein gel (WPG) after 6 min RF heating in the fruit mover placed between a 200 mm RF electrode gap.

(42 °C). As the DPs of two gels were quite different hence heating rates and patterns were expected to be different. Core focused heating occurred in GG fruit whereas surface heating occurred in WPG fruit.

After validation, the computer model was used for simulating the heating profile in the peeled fruits – orange, apple, grapefruit and avocado fruits. As heating of profile of grapefruit was similar to that of orange, grapefruit heating is not shown in Fig. 7 to avoid cluttering and overlapping the figure. It is noticeable that temperature rise in apple was much higher than that in orange. Relatively low heat capacity contributed to the faster RF heating of the apples. The simulation results also suggest core focused heating of peeled orange, grapefruit and apple as occurred in the GG model fruit (Fig. 6). The RF heating profile of avocado complimented that of the WPG model fruit in which subsurface heating occurred. The simulation results were corroborated by the experimental heating profiles of these peeled fruits shown in Fig. 7.

To gain general understanding of the influence of DPs of fruit pulp on heating pattern, simulation was performed to estimated power density at various combinations of dielectric constant and loss factor values. Fig. 8 shows that at a fixed dielectric constant, increasing loss factor increases the power density at fruit core up to a certain loss factor value, and beyond that value further increase in loss factor reduces the power density. In the same graph we can also visualize the effect of the increasing dielectric constant

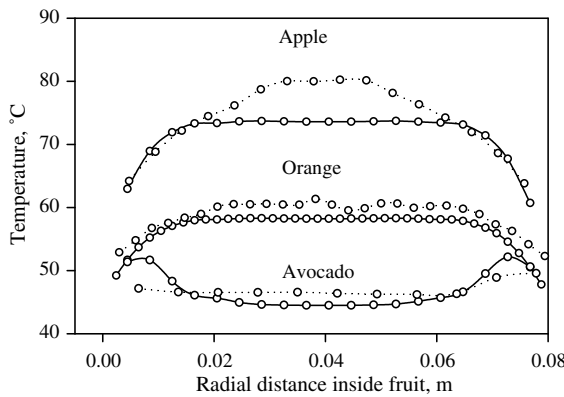


Fig. 7. Simulated (—○—) and experimental (..○..) temperature profile inside a peeled apple, orange and avocado subjected to 6 min RF heating in a water filled container placed between a 200 mm electrode gap.

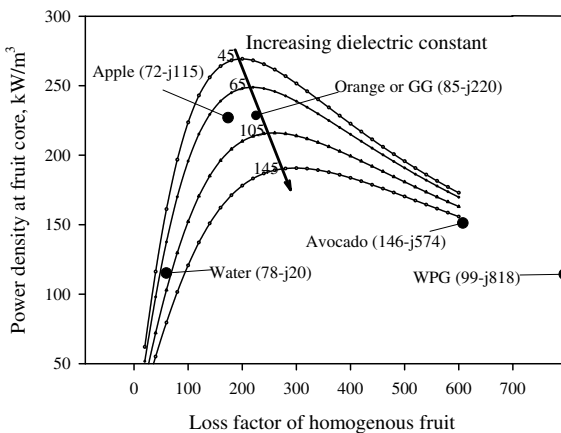


Fig. 8. Simulated effect of dielectric properties on power density at the core of the homogenous fruit (80 mm) assumed to be freely rotating and moving in the water filled container which was sandwiched between two RF electrodes separated by a 200 mm gap. Superimposed dot represents the fresh fruit pulp DPs.

on the power density at the fruit core. Increasing values of dielectric constant reduces the power deposition at the core of the fruit. Each dielectric constant value has its own loss factor value corresponding to peak power density. The loss factor value corresponding to peak power density also shifts to higher side with increasing dielectric constant value (Fig. 8). This fact should explain the faster heating of GG (84-j 220) fruit compared with water (78-j20) and whey protein (99-j818) fruit. In comparison with heating potential of water, higher heating potential of the GG ball resulted in core focused heating whereas lower heating potential of WPG ball led to surface heating. Fig. 8 is helpful to assess the heating uniformity of the homogenous fruits such as peeled fruits.

### 3.3. Effect of peel DPs on heating pattern

WPG model fruit coated with GG was used for validating the modified simulation model and gain understanding of the influence of peel properties on the heating pattern. Fig. 6 shows that the stratified model fruit subjected to RF heating in tap water heated slightly faster than the homogenous WPG ball of the same size (80 mm). As coating of 5 mm thick gellan gel had higher heating potential than the WPG core material, high temperature contours were seen at fruit subsurface. Although, the present model fruit did not represent a real fruit, we could clearly see the effect of the peel properties on the fruit heating pattern. Fig. 9 shows the simulated effect of varying peel DPs on heating potential and pattern. If the ratio of power density of fruit peel and pulp is equal to or less than one, core focused heating may be expected. On the other hand, if the ratio is greater than 1, predominate surface heating may be obtained. Here it should be noted that this condition is based on power density calculation at a particular temperature, whereas the actual temperature profile depends on temperature dependent DPs of individual components along with physical properties such as density, specific heat and thermal conductivity.

Considering all the above factors, RF heating profile of the whole orange was simulated using the properties listed in Table 1 and results are shown in Fig. 10. It is obvious from both simulated and experimental temperature profiles that the differences in both physical and dielectric properties change the heating patterns in the fruit. Using simulated results and observed heating profile in the selected fresh fruit, we will further extend our understanding of RF heating patterns in the fresh fruits in the following section.

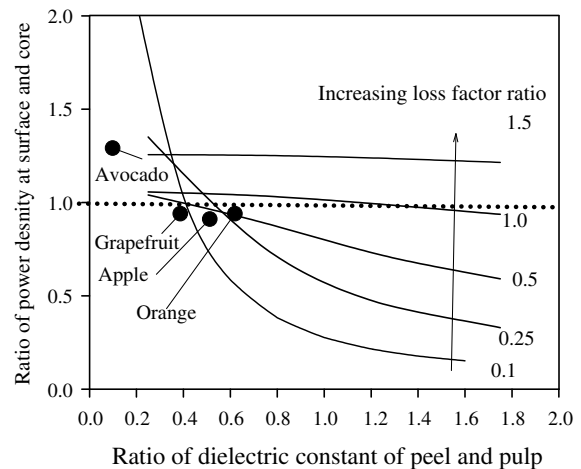
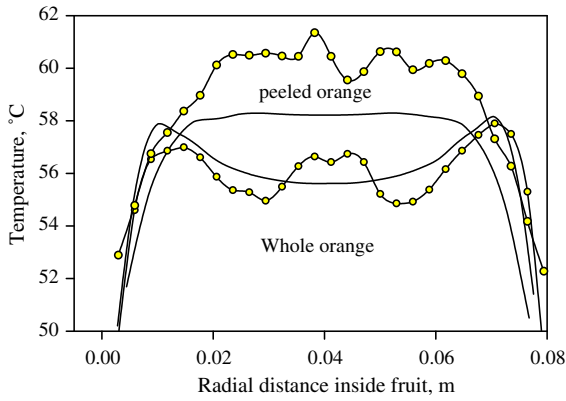


Fig. 9. Simulated effect of dielectric properties ratios (contour as loss factor ratio) of fruit peel (5 mm thick) and pulp on the power density ratio between peel and pulp of the fruit immersed in tap water (DPs:78-j20) and subjected to RF heating in a 200 mm electrode gap. Superimposed dot represents the ratio of pulp and peel DPs of corresponding fresh fruits.



**Fig. 10.** Simulated (—) and experimental (—○—) heating profile over the cross sections of whole and peeled naval orange subjected to 6 min of RF heating in a 200 mm electrode gap.

**3.4. Characterization of RF heating pattern in fresh fruits**

Assorted whole and peeled fruits were subjected to 6 min of RF heating in the tap water filled container placed between 200 mm RF electrodes gap. Initial temperature of all the fruits and water was ~20 °C and final temperature profiles over fruits cross sections, recorded using the infrared imaging camera, are shown in Fig. 11.

In whole naval oranges a temperature gradient was evident with maximum temperature (57 °C) at subsurface and minimum temperature (52 °C) at the fruit core (Fig. 10). However, in peeled

orange, the temperature gradient was reversed with maximum temperature (61 °C) at core and minimum temperature (50 °C) at surface. The DPs of peeled orange were similar to those of the homogeneous GG ball, hence core focused heating occurred as it was observed and simulated for the GG ball. In experimental heating profiles of both whole and peeled oranges, a rise of temperature at the fruit center could be due to presence of air cavity in the orange. In the computer model, we did not consider this small air pocket. Similar to orange, RF heating of whole grapefruit resulted in temperature gradient from outside to inside (Fig. 11), whereas peeled grapefruits were preferentially core heated. It is obvious that significant difference in DPs and of course physical properties of fruits peel and pulp should result in changes in heating pattern. As we saw in Fig. 9 for orange that the ratios of peel and pulp dielectric constant and loss factor were less than 0.5, power density value in peel was comparable to that of pulp. In this case, faster heating of subsurface mainly attributed by lower values of heat capacity and thermal conductivity of peels than that of pulp (Mohsenin, 1980). It is interesting to report that temperature rise was slightly higher (~3 °C) in peeled fruits than that of the whole fruits. This trend might be attributed to different response of the DPs of fruit peel and pulp at elevated temperatures, which in turn influenced heating potential.

Fig. 11 also shows the effect of peel on temperature profiles of golden delicious and red delicious apples. Temperature variation over the cross section of apple was distinct with contour of maximum temperature (~80 °C) at fruit core and minimum temperature (~55 °C) at surface. Similar temperature profile was obtained in simulation using temperature dependent DPs of apple pulp in the computer simulation, but temperature gradient was

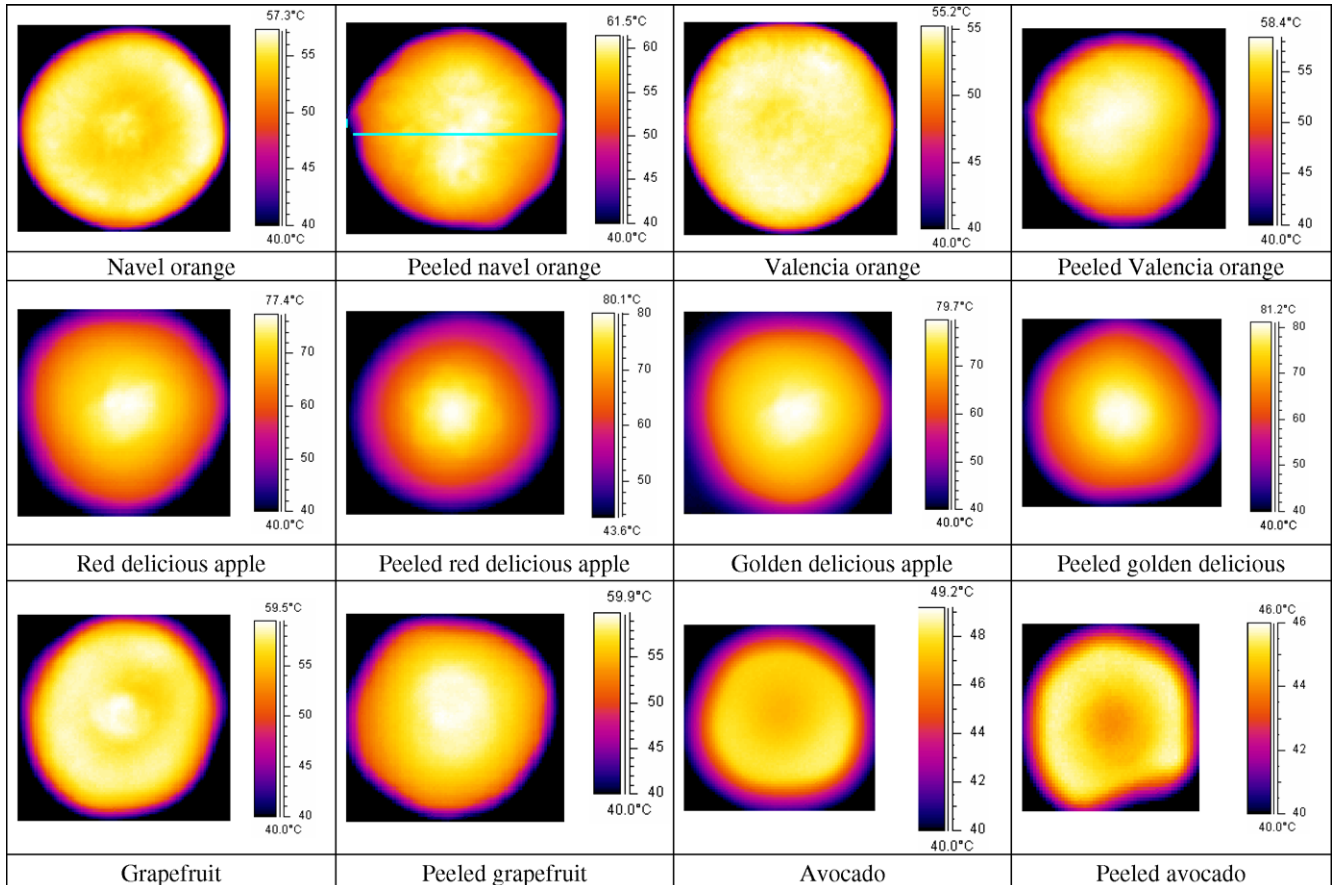


**Fig. 11.** Thermal images showing temperature distribution in fruits subjected to 6 min of RF heating in the fruit mover filled with 20 °C tap water and placed between 200 mm electrode gap.



not that steep as observed in the experimental profile (Fig. 7). In spite of an apparent difference in DPs of pulp and peel of the apples (Fig. 5), influence of peel on heating pattern was not apparent as it was in the oranges. This trend could have been attributed by both very small peel thickness (~2 mm) and gradient of pulp DPs along the radius. The DPs of apple tissues measured at different points on the cross section revealed that the loss factor decreased with the increasing distance of the measurement points apart from the core of the apple (Table 2). In apples, physiological maturity starts from inside, that affects the DPs. Ikediala et al. (2000) measured the DPs of red delicious apple and reported that the dielectric constant of pulp close to the surface was higher than that of the core while the loss factor close to the core higher than that of close to the surface, especially in the RF range.

RF heating pattern in avocado was non-uniform at the core of fruits, i.e. hard pit was at lowest temperature (Fig. 7). Peel removal from the fruit did not make any difference in heating pattern. The loss factor of avocado pulp was more than 600 and dielectric constant value was more than 100, even though a rise in temperature of avocado was (<50 °C) least among all the fruits. The DPs of avocado pulp and WPG ball were in same range hence the heating patterns were comparable.

For fruits such as apple, peaches, which are preferentially core heated, it is an advantage to use RF energy in conjunction with conventional heating. RF assisted hot water heating in which pre-heating of fruits (at certain temperature and for a certain time) in hot water prior to RF heating could be an answer to a quest for an energy efficient, rapid and uniform heating process.

#### 4. Conclusions

In this study DPs of constituent parts of different fruits were measured for characterization of RF heating pattern in fruits. Simulation and experimental RF heating of the fresh fruits indicated that each behaved differently in RF field and heating pattern is influenced by structural parts and their DPs. Based on the peel and pulp DPs we can assess the heating uniformity using a computer model. If the fruits are homogenous and heating potential is more than water, core focused heating should be expected in the fruits during RF heating even after the fruit rotating and moving in the water. In fruits which have thicker peels (e.g. orange and grapefruit), subsurface heating is expected due to difference in dielectric and physical properties of the pulp and the peel.

#### Acknowledgement

This research was supported by Washington State University (WSU) Agricultural Research Center and WSU Impact Centre. The project was also additionally supported by Grants from BARD (US-3276-01), USDA-CSREES (2004-51102-02204) and USDA-NRI (2005-35503-16223).

#### References

Birla, S.L., 2006. Potential of radio frequency heating of fresh fruits as an alternative quarantine method. PhD dissertation: Washington State University, Biological Systems Engineering, Pullman.

Birla, S.L., Wang, S., Tang, J., 2008. Computer simulation of radio frequency heating of model fruit immersed in water. *Journal of Food Engineering* 84 (2), 270–280.

Birla, S.L., Wang, S., Tang, J., Hallman, G., 2004. Improving heating uniformity of fresh fruit in radio frequency treatments for pest control. *Postharvest Biology and Technology* 33, 205–217.

Chen, H., Tang, J., Liu, F., 2007. Coupled simulation of an electromagnetic heating process using the finite difference time domain method. *Journal of Microwave Power and Electromagnetic Energy* 41 (3), 51–60.

Choi, C.T.M., Konrad, A., 1991. Finite-Element modeling of the RF heating process. *IEEE Transactions on Magnetics* 27 (5), 4227–4230.

Foster, K.R., Schwan, H.P., 1989. Dielectric properties of tissues and biological materials: a critical review. *Critical Review of Biomedical Engineering* 17 (1), 25–104.

Guan, D., Cheng, M., Wang, Y., Tang, J., 2004. Dielectric properties of mashed potatoes relevant to microwave and radio-frequency pasteurization and sterilization processes. *Journal of Food Science* 69 (1), E30–E37.

Hallman, G.J., Sharp, J.L., 1994. Radio frequency heat treatments. In: *Quarantine Treatments for Pests of Food Plants*. Westview Press, San Francisco, CA, pp. 165–170.

Hewlett & Packard, 1996. HP 85070B Dielectric Probe Kit User's Manual, Agilent Technologies, Palo Alto.

Ikediala, J.N., Hansen, J.D., Tang, J., Drake, S.R., Wang, S., 2002. Development of a saline water immersion technique with RF energy as a postharvest treatment against codling moth in cherries. *Postharvest Biology and Technology* 24, 25–37.

Ikediala, J.N., Tang, J., Drake, S.R., Neven, L.G., 2000. Dielectric properties of apple cultivars and codling moth larvae. *Transactions of the ASAE* 43 (5), 1175–1184.

Ikediala, J.N., Tang, J., Neven, L.G., Drake, S.R., 1999. Quarantine treatment of cherries using 915 MHz microwaves: temperature mapping, codling moth mortality and fruit quality. *Postharvest Biology and Technology* 16 (2), 127–137.

Mohsenin, N.N., 1980. *Thermal Properties of Foods and Agricultural Materials*. CRC Press, New York.

Nelson, S.O., 1996. Review and assessment of radio-frequency and microwave energy for stored-grain insect control. *Transactions of the ASAE* 39 (4), 1475–1484.

Nelson, S.O., 2003. Frequency and temperature dependent permittivity of fresh fruits and vegetables from 0.01 to 1.8 GHz. *Transactions of the ASAE* 46 (2), 567–574.

Rehman, S., 1995. *Food Properties Handbook*. CRC Press, New York.

Ryynänen, S., 1995. The electromagnetic properties of food materials: a review of the basic principles. *Journal of Food Engineering* 29, 409–429.

Seaman, R., Seals, J., 1991. Fruit pulp and skin dielectric properties for 150 to 6400 MHz. *Journal of Microwave Power and Electromagnetic Energy* 26, 72–81.

Sipaghioglu, O., Barringer, S.A., 2003. Dielectric properties of vegetables and fruits as a function of temperature, ash, and moisture content. *Journal of Food Science* 68 (1), 234–239.

Tang, J., 2005. Dielectric properties of foods. In: *The Microwave Processing of Foods*. Woodhead, Cambridge.

Tang, J., Ikediala, J.N., Wang, S., Hansen, J.D., Cavalieri, R.P., 2000. High-temperature-short-time thermal quarantine methods. *Postharvest Biology and Technology* 21 (1), 129–145.

Tang, J., Tung, M.A., Zeng, Y., 1995. Mechanical properties of gellan gels in relation to divalent cations. *Journal of Food Science* 60 (4), 748–752.

Tang, J., Tung, M.A., Zeng, Y., 1997. Gelling properties of gellan solutions containing monovalent and divalent cations. *Journal of Food Science* 62 (4), 688–692, 712.

Venkatesh, M.S., Raghavan, G.S.V., 2004. An overview of microwave processing and dielectric properties of agri-food materials. *Biosystems Engineering* 88 (1), 1–18.

Wang, S., Birla, S.L., Tang, J., Hansen, J.D., 2006. Postharvest treatment to control codling moth in fresh apples using water assisted radio frequency heating. *Postharvest Biology and Technology* 40 (1), 89–96.

Wang, S., Ikediala, J.N., Tang, J., Hansen, J.D., Mitcham, E., Mao, R., Swanson, B., 2001a. Radio frequency treatments to control codling moth in in-shell walnuts. *Postharvest Biology and Technology* 22 (1), 29–38.

Wang, S., Monzon, M., Gazit, Y., Tang, J., Mitcham, E.J., Armstrong, J.W., 2005. Temperature-dependent dielectric properties of selected subtropical and tropical fruits and associated insect pests. *Transactions of the ASAE* 48 (5), 1873–1881.

Wang, S., Monzon, M., Johnson, J.A., Mitcham, E.J., Tang, J., 2007. Industrial-scale radio frequency treatments for insect control in walnuts II: Insect mortality and product quality. *Postharvest Biology and Technology* 45 (2), 247–253.

Wang, S., Tang, J., Cavalieri, R.P., 2001b. Modeling fruit internal heating rates for hot air and hot water treatments. *Postharvest Biology and Technology* 22 (3), 257–270.

Wang, S., Tang, J., Cavalieri, R.P., Davis, D.C., 2003a. Differential heating of insects in dried nuts and fruits associated with radio frequency and microwave treatments. *Transactions of the ASAE* 46 (4), 1175–1182.

Wang, S., Tang, J., Johnson, J.A., Mitcham, E., Hansen, J.D., Hallman, G., Drake, S.R., Wang, Y., 2003b. Dielectric properties of fruits and insect pests as related to radio frequency and microwave treatments. *Biosystems Engineering* 85 (2), 201–212.

Wang, Y.F., Wig, T.D., Tang, J.M., Hallberg, L.M., 2003c. Dielectric properties of foods relevant to RF and microwave pasteurization and sterilization. *Journal of Food Engineering* 57 (3), 257–268.